Radiation Boundary Conditions for Numerical Simulation of Transmission Problems in Acoustics

Hongrui Geng, Zhaoran Wang, and Zhenhua Xu

***Abstract*—In this paper, the classical two-dimensional Helmholtz transmission problem is reduced to a local boundary value problem by introducing an artificial boundary. A localized Dirichlet-to-Neumann (DtN) mapping is defined on the artificial boundary. Then the variational equations and Galerkin formulation are derived. The effectiveness of the methods is demonstrated using various numerical examples.**

***Index Terms*—acoustic transmission problem, Finite element method, Radiation Boundary Conditions, Hankel function, weak formulation.**

I. Introduction

In order to solve the Helmnoltz transmission problem in an infinite domain, many numerical methods have been proposed by many researchers. One of the most conventional numerical methods for solving scattering problems with constant parameters is to reformulate the transmission problem as a system of BIE over the boundary of the obstacle [1], [2], [3], [4], [5]. The second approach is the perfectly matched layer (PML) method [6], [7], which is to surround the computational domain by a layer of finite thickness with specially designed medium that would either slow down or attenuate all the waves that propagate from the inside computational domain. This approach is easy to implement and is very effective. Another popular conventional method for the transmission problem is the coupling of finite element method (FEM) and the boundary element method (BEM). The common method is to introduce an enough big artificial boundary enclosing the obstacle inside and impose an appropriate artificial boundary condition. Then one can apply FEM to solve the Helmholtz equation on the bounded domain and BEM to solve the exterior value problem outside artificial boundary, respectively. Many authors realized the coupling procedure to exterior transmission problem by defined a Dirichlet-to-Neumann (DtN) mapping on the artificial boundary [8], [9], [10], [11], [12], [13]. The authors of [12], [13], [14], [15] define it by some basic boundary integral operators, whereas some researchers represent the DtN mapping through Fourier expansion series [8], [9], [16], [17], [18], [11]. The authors of [19], [20], [21], [22] make an extension of the standard DtN-FEM on general artificial boundary. But these exact boundary conditions are given in an infinite series which must be truncated in actual computation and also some significant error will appear in this case. Moreover, the exact boundary condition is nonlocal, and result the dense blocks of linear equations. Due to this, we consider local approximate boundary conditions.

There are many types of local boundary conditions. The simplest local boundary condition is the Sommerfeld condition. Engquis and Majda [23], [24] developed a sequence of local boundary conditions on the basis of factorization of pseudodifferential operators. Bayliss and Turkel [25] proposed another family of local boundary conditions, based on the asymptotic approximation of the solution of the wave equation. As for the numerical investigation of local boundary conditions, Shirron and Babuska [26] compared the performance and accuracy for various local boundary conditions. In this paper, we deal with the two-dimensional transmission problem in acoustics by the localization procedure initially proposed by Feng in [9]. We reduce the classical transmission problem to a local boundary value problem by defined a local DtN mapping. Then by using the technique in [27] for interior acoustic transmission problem, we show that the corresponding variational problem of the local boundary value problem.

The organization of the paper is as follows: In Section 2, we describe the classical Helmholtz transmission problem. In Section 3, we reduce the transmission problem in acoustics to a local boundary value problem. Then, we discuss the corresponding variational equations and modified formulation in Section 4. In the last section, we present some numerical experiments to illustrate efficiency of the proposed method.

II. Statement of the problem

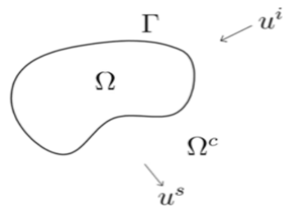

Fig. 1. Boundary value problem (1)-(5).

Let Ω denote a bounded domain with smooth boundary Γ, and let $\Omega^c = \mathbb{R}^2/\overline{\Omega}$ be the unbounded exterior domain in $\mathbb{R}^2$(see Fig. 1). We consider the following boundary value problem in acoustics: Given the incident field u^i, find the total field $u \in C^2(\Omega) \cap C^1(\overline{\Omega})$ and the scattered field $u^s \in$

Manuscript received September 5, 2021; revised January 22, 2022. This work was supported by the National Natural Science Foundation of China (11701526,11971446), 2016 PhD Start-up Project of Zhengzhou University of Light Industry (2016BSJJ050), Excellent Young Scholars Foundation of Zhengzhou University of Light Industry.

Hongrui Geng (Corresponding author) is a Lecturer of College of Mathematics and Information Science, Zhengzhou University of Light Industry, Zhengzhou 450002, China. (e-mail: ghr0313@hotmail.com).

Zhaoran Wang is a Master candidate of College of Mathematics and Information Science, Zhengzhou University of Light Industry, Zhengzhou 450002, China. (e-mail: zhaoran.Wang@hotmail.com).

Zhenhua Xu is an Associate professor of College of Mathematics and Information Science, Zhengzhou University of Light Industry, Zhengzhou 450002, China. (e-mail: xuzhenhua19860536@163.com).

$C^2(\Omega^c) \cap C^1(\overline{\Omega^c})$ satisfying

$$\Delta u + k_1^2 u = 0, \quad \text{in } \Omega, \tag{1}$$
$$\Delta u^s + k_2^2 u^s = 0, \quad \text{in } \Omega^c, \tag{2}$$
$$u = u^s + u^i, \quad \text{on } \Gamma, \tag{3}$$
$$\frac{\partial u}{\partial \nu} = \frac{\partial u^s}{\partial \nu} + \frac{\partial u^i}{\partial \nu}, \text{ on } \Gamma, \tag{4}$$

where $k_j \neq 0$, $j = 1, 2$, are wave numbers with $\mathrm{Im}(k_j) \geq 0$, ν denotes the outer unit normal to the boundary and $\partial/\partial\nu$ means the normal derivative on Γ point from Ω to Ω^c. The derivation of these bounary condition by an appropriate normalization can be found in [28]. Moreover, for the uniqueness, the scattering field u^s has to satisfy the standard *Sommerfeld* radiation condition

$$\lim_{r\to\infty} r^{\frac{1}{2}}(\frac{\partial u^s}{\partial r} - ik_2 u^s) = 0 \tag{5}$$

with $i = \sqrt{-1}, r = |x|$ and $x = (x_1, x_2) \in \mathbb{R}^2$.

In order to obtain the uniqueness result of the transmission problem, it needs to add some restrictions on the wave number k_1 and k_2. Such constraints of wave numbers are summarized in the following theorem.

Theorem 2.1: Let $k_2 \neq 0$ be such that $\mathrm{Im}(k_2) \geq 0$, and let $k_1 \neq 0$ be such that $\mathrm{Im}(k_1^2\overline{k_2}) \geq 0$. Then the classical transmission problem (1)-(5) has at most one solution.

A proof of the above theorem can be found in [3].

III. Localization of the boundary value problem

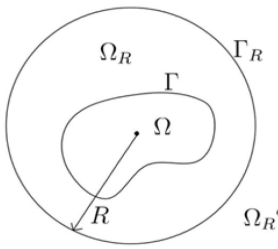

Fig. 2. Local boundary value problem (10)-(14)

We introduce in this section a local boundary value problem in Ω_R with the localized boundary condition on Γ_R (see Fig. 2). We describe the localization procedure initially proposed in [9], which is actually the one most correlated with the exact DtN mapping T. In [9], with a simple manipulation, the normal derivative of u^s on Γ_R

$$\frac{\partial u^s}{\partial r}(R,\theta) = \sum_{n=0}^{\infty}{}' k_2 H_n^{(1)'}(k_2R)(a_n\cos(n\theta) + b_n\sin(n\theta)) \tag{6}$$

can be written as

$$\frac{\partial u^s}{\partial r}(R,\theta) = \sum_{n=0}^{\infty}{}' \frac{k_2 H_n^{(1)'}(k_2R)}{H_n^{(1)}(k_2R)} H_n^{(1)}(k_2R)(a_n\cos(n\theta) + b_n\sin(n\theta)), \tag{7}$$

for $\forall u \in H^s(\Gamma_R)$, $s \geq 1/2$. Here and throughout the presentation, the prime behind the summation means that the first term in the summation is multiplied by 1/2. By assuming that k_2R being sufficiently large and applying the asymptotic expansion of the Hankel function in (7), we can obtain that

$$\frac{k_2 H_n^{(1)'}(k_2R)}{H_n^{(1)}(k_2R)} \sim ik_2 \sum_{m=0}^{\infty}(\frac{i}{2k_2R})^m c_m(n^2), \tag{8}$$

where the coefficients c_m are defined recursively:

$$\begin{aligned} c_0(n^2) =& c_1(n^2) = 1,\\ c_2(n^2) =& 2(n^2 - \frac{1}{4}),\\ &\dots\dots\\ c_k(n^2) =& (2k-2)(n,k-1) - c_2(n^2)(n,k-2) - \cdots\\ &- c_{k-1}(n^2)(n,1), \quad k = 0,1,2...m. \end{aligned}$$

here

$$(n,m) = \frac{1}{m!}\prod_{k=1}^{m}\left(n^2 - \left(\frac{2k-1}{2}\right)^2\right)$$

is an even polynomial in n of degree $2m$.

Because n^2 can be regarded as eigenvalues of u^s corresponding to the operator $-\partial^2/\partial\theta^2$, we can interchange the order of summations as substituting (8) into (7). Hence, we have

$$\begin{aligned} &\frac{\partial u^s}{\partial r}(R,\theta)\\ =&\sum_{n=0}^{\infty}{}' \frac{k_2 H_n^{(1)'}(k_2R)}{H_n^{(1)}(k_2R)} H_n^{(1)}(k_2R)(a_n\cos(n\theta) + b_n\sin(n\theta))\\ \sim&\sum_{n=0}^{\infty}{}' ik_2 \sum_{m=0}^{\infty}(\frac{i}{2k_2R})^m c_m(n^2) H_n^{(1)}(k_2R)(a_n\cos(n\theta)\\ &+ b_n\sin(n\theta))\\ =&ik_2\sum_{m=0}^{\infty}(\frac{i}{2k_2R})^m c_m(-\frac{\partial^2}{\partial\theta^2})\sum_{n=0}^{\infty}{}' H_n^{(1)}(k_2R)(a_n\cos(n\theta)\\ &+ b_n\sin(n\theta))\\ =&ik_2\sum_{m=0}^{\infty}(\frac{i}{2k_2R})^m c_m(-\frac{\partial^2 u^s}{\partial\theta^2}). \end{aligned}$$

Thus the localized DtN mapping $S : H^s(\Gamma_R) \mapsto H^{s-1}(\Gamma_R), \forall\, \varphi \in H^s(\Gamma_R),\ 1/2 \leq s \in \mathbb{R}$, is defined as

$$S\varphi := ik_2\sum_{m=0}^{\infty}(\frac{i}{2k_2R})^m c_m(-\frac{\partial^2\varphi}{\partial\theta^2}), \tag{9}$$

here S is a bounded linear operator. Now we can reduce the boundary value problem (1)-(5) to the following local boundary value problem: Given the incident field u^i, find $u \in C^2(\Omega) \cap C^1(\overline{\Omega})$ and $u^s \in C^2(\Omega_R) \bigcap C^1(\overline{\Omega_R})$ such that

$$\Delta u + k_1^2 u = 0 \quad \text{in } \Omega, \tag{10}$$
$$\Delta u^s + k_2^2 u^s = 0 \quad \text{in } \Omega_R, \tag{11}$$
$$u = u^s + u^i \quad \text{on } \Gamma, \tag{12}$$
$$\frac{\partial u}{\partial \nu} = \frac{\partial u^s}{\partial \nu} + \frac{\partial u^i}{\partial \nu} \quad \text{on } \Gamma, \tag{13}$$
$$\frac{\partial u^s}{\partial \nu} = Su^s \quad \text{on } \Gamma_R. \tag{14}$$

The localized DtN mapping S and the truncated localized DtN mapping S^M can be written as

$$S = \sum_{m=0}^{\infty} S_m \quad (15)$$

and

$$S^M = \sum_{m=0}^{M} S_m. \quad (16)$$

respectively. Here M is the truncation order of S. The first four terms of S read as

$$S_0 = ik_2,\ S_1 = -\frac{1}{2R},$$
$$S_2 = \frac{i}{8k_2R^2} + \frac{i}{2k_2R^2}\frac{\partial^2}{\partial\theta^2},$$
$$S_3 = \frac{1}{8(k_2)^2R^3} + \frac{1}{2(k_2)^2R^3}\frac{\partial^2}{\partial\theta^2}.$$

In particular, the first term S_0 gives the approximated Sommerfeld condition.

IV. Weak formulation

In this section, we study the weak formulation of (10)-(14). We first introduce the Sobolev spaces

$$\mathcal{H}^t = H^t(\Omega) \times H^t(\Omega_R), \quad (17)$$
$$\mathcal{H}^t_\Gamma = \{(v_1, v_2) \in \mathcal{H}^t,\ v_1 = v_2 \text{ on } \Gamma\}, \quad (18)$$

equipped with the norm

$$\|V\|_{\mathcal{H}^t} = \left(\|v_1\|^2_{H^t(\Omega)} + \|v_2\|^2_{H^t(\Omega_R)}\right)^{1/2},$$

$\forall\ V = (v_1, v_2) \in \mathcal{H}^t$. The standard weak formulation of the nonlocal boundary value problem (10)-(14) reads: Given u^i, find $U = (u, u^s) \in \mathcal{H}^1$ such that

$$u - u^s = u^i \quad \text{on} \quad \Gamma$$

and

$$A(U,V) = a_1(u, v_1) + a_2(u^s, v_2) + b(u^s, v_2) = \ell(V), \quad (19)$$

for any $V = (v_1, v_2) \in \mathcal{H}^1_\Gamma$, where

$$a_1(u, v_1) = \int_\Omega \nabla u \cdot \nabla \bar{v}_1 dx - k_1^2 \int_\Omega u\bar{v}_1 dx, \quad (20)$$
$$a_2(u^s, v_2) = \int_{\Omega_R} \nabla u^s \cdot \nabla \bar{v}_2 dx - k_2^2 \int_{\Omega_R} u^s\bar{v}_2 dx, \quad (21)$$
$$b(u^s, v_2) = -\int_{\Gamma_R} (Su^s)\bar{v}_2 ds, \quad (22)$$
$$\ell(V) = \int_\Gamma \frac{\partial u^i}{\partial \nu}\bar{v}_1 ds. \quad (23)$$

Here, $a_1(u, v_1)$ is a sesquilinear form defined on $H^1(\Omega) \times H^1(\Omega)$, $a_2(u^s, v_2)$ and $b(u^s, v_2)$ are sesquilinear forms defined on $H^1(\Omega_R) \times H^1(\Omega_R)$, and $\ell(V)$ is a linear functional dependent on $\partial u^i/\partial\nu \in H^{-1/2}(\Gamma)$.

Lemma 4.1: The sesquilinear form A is continuous, i.e.,

$$|A(U,V)| \leq c\|U\|_{\mathcal{H}^1}\|V\|_{\mathcal{H}^1}, \quad \forall\ U, V \in \mathcal{H}^1_\Gamma, \quad (24)$$

and satisfies the Gårding's inequality taking the form

$$Re\{A(V,V)\} \geq \alpha\|V\|^2_{\mathcal{H}^1} - \beta\|V\|^2_{\mathcal{H}^{1/2+\epsilon}}, \quad \forall\ V \in \mathcal{H}^1_\Gamma, \quad (25)$$

where $c > 0$, $\alpha > 0$, $\beta \geq 0$, $1/2 > \epsilon > 0$ are all constants independent of U and V.

A. Modified weak formulation

We consider the modified variational equation of (19)-(23) for $U = (u, u^s) \in \mathcal{H}^1$,

$$A^M(U,V) = a_1(u,v) + a_2(u^s,\nu) + b^M(u^s,\nu) = \ell(v), \quad (26)$$

$\forall\ V = (v,\nu) \in \mathcal{H}^1_\Gamma$, where $b^M(u^s,\nu) = -\int_{\Gamma_R}(S^M u^s)\bar{\nu} ds$.

B. Galerkin formulation

Let $\mathcal{H}_h = (S_h, S_h^s)$ be the standard finite element space. Now we consider the Galerkin formulation of (26): Given u^i, find $U_h = (u_h, u_h^s) \in \mathcal{H}^h \subset \mathcal{H}^1$ satisfying

$$A^M(U_h, V_h) = a_1(u_h, v_h) + a_2(u_h^s, \nu_h) + b^M(u_h^s, \nu_h) = \ell(v_h), \quad (27)$$

$\forall\ V_h = (v_h, \nu_h) \in \mathcal{H}^h_\Gamma$.

It can be shown that the discrete sesquilinear form satisfies the BBL-condition as follows [29] :

Lemma 4.2: Under the same assumptions on k_1 and k_2 as in Theorem 2.1, suppose that the finite element space $\mathcal{H}^h_\Gamma \subset \mathcal{H}^1_\Gamma$ satisfies the standard approximation property, then there exist constants $M_0 \geq 0$ and $h_0 > 0$ such that $A^M(V,W)$ for $0 < h \leq h_0$, $M \geq M_0$ satisfies the BBL condition in the form

$$\sup_{(0,0)\neq W_h \in \mathcal{H}^h_\Gamma} \frac{|A^N(V_h, W_h)|}{\|W_h\|_{\mathcal{H}^1}} \geq \gamma\|V_h\|_{\mathcal{H}^1}, \quad \forall\ V_h \in \mathcal{H}^h_\Gamma. \quad (28)$$

Here, $\gamma > 0$ is the inf-sup constant independent of h.

V. Numerical experiments

In this section, we present several numerical tests to validate our theoretical results.

A. A model problem

We compute the scattering problem by an infinite circular cylinder of radius R_0, of a plane wave $u^i = e^{ik_2 x\cdot d}$ propagating along the positive x_1 axis with the transmission boundary condition on Γ. Here $x = (x_1, x_2)$ and $d = (1, 0)$ is the unit vector describing the traveling direction of the incident wave. The mathematical model can be formulated as the transmission problem (1)-(5) with the interface Γ to be a circle of radius R_0. In this case, the exact solutions u and u^s of (1)-(5) can be written as

$$u(r,\theta) = \sum_{n\in\mathbb{Z}} a_n J_n(k_1 r)e^{in\theta}, \quad \forall\ r \leq R, \quad (29)$$
$$u^s(r,\theta) = \sum_{n\in\mathbb{Z}} b_n H_n^{(1)}(k_2 r)e^{in\theta}, \quad \forall\ r \geq R, \quad (30)$$

where $J_n(\cdot)$ denotes the Bessel function of the first kind, $H_n^{(1)}(\cdot)$ the Hankel function of the first kind, and a_n as well as b_n are Fourier coefficient of u and u^s on Γ respectively. In terms of the Jacobi-Anger expansion formula under the polar coordinates for the plane wave

$$u^i(r,\theta) = e^{ik_2 r cos\theta} = \sum_{n\in\mathbb{Z}} i^n J_n(k_2 r)e^{in\theta}, \quad (31)$$

we can obtain a_n and b_n in (29) and (30) explicitly by

$$a_n = \frac{i^n k_2(J_n'(k_2R_0)H_n^{(1)}(k_2R_0) - J_n(k_2R_0)H_n^{(1)'}(k_2R_0))}{k_1J_n'(k_1R_0)H_n^{(1)}(k_2R_0) - k_2J_n(k_1R_0)H_n^{(1)'}(k_2R_0)}, \tag{32}$$

$$b_n = \frac{i^n(k_2J_n'(k_1R_0)J_n(k_1R_0) - k_1J_n'(k_1R_0)J_n(k_2R_0))}{k_1J_n'(k_1R_0)H_n^{(1)}(k_2R_0) - k_2J_n(k_1R_0)H_n^{(1)'}(k_2R_0)}. \tag{33}$$

Here the prime behind Bessel and Hankel functions denotes the first order derivative. In the following simulations, the infinite Fourier series (29) and (30) are truncated when the relative change because of an additional mode in the fields is below 10^{-6}.

We add the artificial boundary Γ_R to be a circle of radius R. It enclose the circle of radius R_0 with the same center as Γ. Hence, the computational region Ω_R is the annulus between Γ and Γ_R (see Fig. 3).

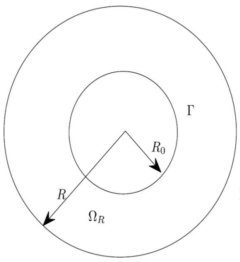

Fig. 3. Computational domain of the model problem.

To find the finite element solution of (27), we need to numerically compute the sesquilinear form

$$b(u^s, \nu) = -\int_{\Gamma_R} (S^M u^s)\bar{\nu} ds \tag{34}$$

In what follows, some numerical examples using linear Lagrange elements are presented. We generate an initial coarse triangular mesh using the MATLAB PDEtool and uniformly refine the mesh to perform a convergence study. Moreover, we always set the radius $R_0 = 1$, the wave number $k_1 = 1$ unless otherwise stated.

Experiment 1. In this test, we consider local boundary value problem by the truncated localized DtN mpping S^M in (16). In (34), we choose $M = 3$, $k_2 = 2$, $R = 10$ and compute the solutions for different h . From Fig. 4, we can find that the numerical solutions is almost the same as the exact solutions when $h = 0.1399$. Table I implies the convergence order

$$\|U - U_h\|_{\mathcal{H}^0} = O(h_F^2), \quad \|U - U_h\|_{\mathcal{H}^1} = O(h_F), \tag{35}$$

where $U = (u, u^s)$ and $U_h = (u_h, u_h^s)$, h_F is the finite element meshsize.

TABLE I
NUMERICAL ERRORS WHEN $R_0 = 1, R = 10$.

h	$\mathcal{H}^0$-norm	order	$\mathcal{H}^1$-norm	order
2.1674	4.4979E+0		1.0350E+1	
1.0852	2.2710E+0	0.99	5.8138E+0	0.83
0.5523	6.3913E-1	1.88	2.1859E+0	1.45
0.2785	1.6650E-1	1.96	9.2622E-1	1.25
0.1399	4.2380E-2	1.99	4.3686E-1	1.09

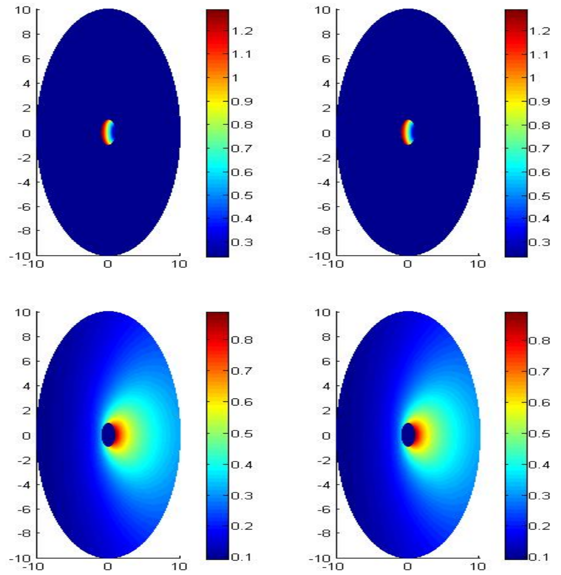

Fig. 4. Absolute values of the exact solutions (left) and the numerical solutions (right) of u (top)and u^s(bottom) for Experiment 1.

Experiment 2. We compute the model problem to examine the dependence of numerical errors on domain discretization , and use different wave numbers $k_2 = 2, 4, 6$. Moreover, we still choose $R = 10$. Fig. 5 is presented to show the log-log plot of errors of U measured in $\mathcal{H}^0$-norm and $\mathcal{H}^1$-norm respect to $1/h$ (h is the meshsize) and verifies that the optimal order of convergence has been observed.

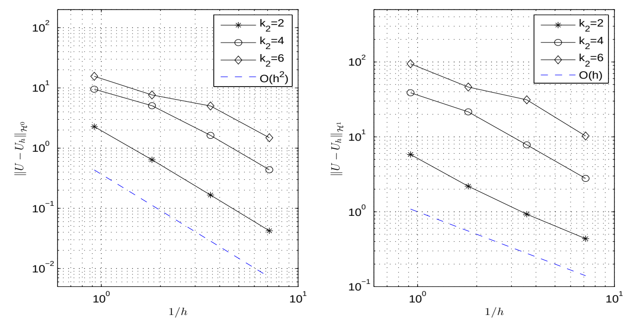

Fig. 5. Log-log plots for numerical errors (vertical) of U vs. $1/h$ (horizontal). Left: $\mathcal{H}^0$-norm; right: $\mathcal{H}^1$-norm.

Experiment 3. We compute the finite element solution of (10)-(14) with the third order local boundary condition ($M = 3$). We choose the wave number $k_2 = 2$, and consider four different values of radius $R = 2, 4, 7, 10$ respectively. Numerical errors in $\mathcal{H}^0$-norm on Γ are presented in Fig. 6 indicating that there is no improvement of accuracy in the case that $k_2R = 4$ and a limited improvement of accuracy in the case that $k_2R = 8$, as the finite element mesh is refined. However, significant improvements of accuracy are obtained when $k_2R = 14$ as the mesh is refined. The error in $\mathcal{H}^0$-norm is roughly of $O(h^2)$ when $R = 10$. This fact is in good agreement with the assumptions for the derivation of the local boundary conditions. Therefore, to reduce the error, one has to place the artificial boundary at some distance away from the scatterer as the wave number k_2 is small.

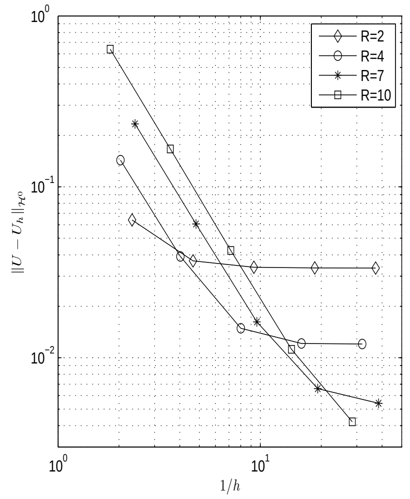

Fig. 6. Log-log plot vs. $1/h$ for errors in $\mathcal{H}^0$-norm(left) for a plane wave.

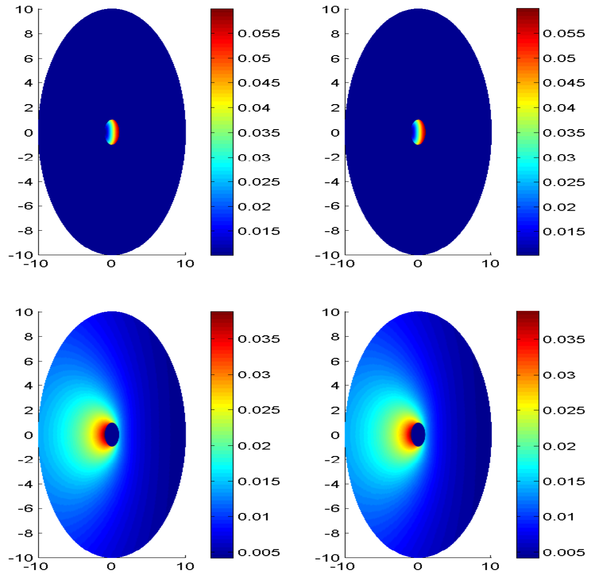

Fig. 7. Absolute values of the exact solutions (left) and the numerical solutions (right) of u (top)and u^s(bottom) for Experiment 4.

B. Another model problem

Next, we consider a point source $u^i = \frac{i}{4}H_0^{(1)}(k_2|x - x_0|)$ located at $x_0 \in \mathbb{R}^2 \backslash \overline{\Omega}$. It can be expanded as

$$u^i(r, \theta) = \frac{i}{4}\sum_{n\in\mathbb{Z}} H_n^{(1)}(k_2|x_0|)J_n(k_2 r)e^{in\theta}, \qquad (36)$$

In this case, exact solutions u and u^s of (1)-(5) also can be written as (29) and (30) respectively, where the Fourier coefficients a_n and b_n are given explicitly by

$$a_n = \frac{b_n H_n^{(1)}(k_2R_0) + \frac{i}{4}H_n^{(1)}(k_2|x_0|)J_n(k_2R_0)}{J_n(k_1R_0)}, \qquad (37)$$

$$b_n = \frac{i}{4}\Big(\frac{k_2H_n^{(1)}(k_2|x_0|)J_n'(k_2R_0)J_n(k_1R_0)}{k_1H_n^{(1)}(k_2R_0)J_n'(k_1R_0) - k_2H_n^{(1)'}(k_2R_0)J_n(k_1R_0)} - \frac{k_1H_n^{(1)}(k_2|x_0|)J_n(k_2R_0)J_n'(k_1R_0)}{k_1H_n^{(1)}(k_2R_0)J_n'(k_1R_0) - k_2H_n^{(1)'}(k_2R_0)J_n(k_1R_0)}\Big). \qquad (38)$$

Here the prime behind Bessel and Hankel functions denotes the first order derivative. In the following examples, we choose $k_1 = 1$, $R_0 = 1$, $x_0 = (2, 0)$.

Experiment 4. Let $k_2 = 2$, $R = 10$, and we compute the solutions for different h and present the solutions in Fig. 7 when $h = 0.1399$.

Experiment 5. We choose the third order truncated localized DtN mapping and let $k_2 = 2$, $R = 2$ and 10, respectively. Numerical errors and convergence order are presented in Table II ($R = 2$) and in Table III ($R = 10$). In particular, there is no apparent improvement as we refine the mesh for the case that $k_2R = 4$. This fact implies the value of k_2R must be large enough for the validation of asymptotic expansion.

TABLE II
NUMERICAL ERRORS WHEN $R_0 = 1, R = 2$.

h	$\mathcal{H}^0$-norm	order	$\mathcal{H}^1$-norm	order
0.4304	6.7210E-3		6.9834E-2	
0.2152	3.8159E-3	0.82	3.5810E-2	0.96
0.1076	3.4898E-3	0.13	1.8891E-2	0.92
0.0538	3.4588E-3	0.013	1.1103E-2	0.77
0.0269	3.4546E-3	0.002	8.0426E-3	0.47

TABLE III
NUMERICAL ERRORS WHEN $R_0 = 1, R = 10$.

h	$\mathcal{H}^0$-norm	order	$\mathcal{H}^1$-norm	order
2.1674	1.9857E-1		4.5857E-1	
1.0852	1.0585E-1	0.91	2.6860E-1	0.77
0.5523	3.0298E-2	1.85	1.0071E-1	1.45
0.2785	7.9075E-3	1.96	4.2116E-2	1.27
0.1399	2.0146E-3	1.99	1.9742E-2	1.10

VI. Conclusion

In this paper, we used a DtN Finite element method (DtN-FEM) based on localized DtN mapping to solve the classical two-dimensional Helmholtz transmission problem. Based on the asymptotic expansion of Hankel functions for large arguments, an approach for the construction of localized DtN mapping is suggested and gives expression of the normal derivative at spherical artificial boundary in terms of linear combination of Laplace-Beltrami operator and its iterates, i.e. tangential derivatives of even order exclusively. Then the variational equations and Galerkin formulation are derived. Numerical results are presented to demonstrate the efficiency and accuracy of the schemes.

References

[1] M. Costabel, E. Stephan, "A direct boundary integral equation method for transmission problems," *Journal of Mathematical Analysis and Applications*, vol. 106, pp. 367-413, 1985.
[2] G.C. Hsiao, L. Xu, "A system of boundary integral equations for the transmission problem in acoustics," *Applied Numerical Mathematics*, vol. 61, pp. 1017-1029, 2011.
[3] R.E. Kleinman, P.A. Martin, "On single integral equations for the transmission problem of acoustics," *SIAM Journal on Applied Mathematics.*, vol. 48, no. 2, pp. 307-325, 1988.
[4] ML. Rapún, FJ. Sayas, "Mixed boundary integral methods for Helmholtz transmission problems," *Journal of Computational and Applied Mathematics*, vol. 214, pp. 238-258, 2008.
[5] T. Yin, GC. Hsiao, L. Xu, "Boundary integral equation methods for the two dimensional fluid-solid interaction problem," *SIAM Journal on Numerical Analysis*, vol. 55, pp. 2361-2393, 2017.
[6] J. Bérenger, "A perfectly matched layer for the absorption of electromagnetic waves," *Journal of Computational physics*, vol. 114, pp. 185-200, 1994.

[7] Z. Chen, X. Liu, "An adaptive perfectly matched technique for time-harmonic scattering problems," *SIAM Journal on Numerical Analysis*, vol. 43, pp. 645-671, 2005.
[8] K. Feng, "Finite element method and natural boundary reduction," in *Proceedings of the International Congress of Mathematicians, Warsaw,* pp. 1439-1453, 1983.
[9] K. Feng, "Asymptotic radiation conditions for reduced wave equation," *Journal of Computational Mathematics*, vol. 2, pp. 130-138, 1984.
[10] D. Givoli, "Numerical methods for problems in infinite domains," *Elsevier Scientific Publishing Co.*, vol. 33, 1992.
[11] G.C. Hsiao, N. Nigam, J. Pasciak, L. Xu, "Error analysis of the DtN-FEM for the scattering problem in acoustics via Fourier analysis," *Journal of Computational and Applied Mathematics*, vol. 235, pp. 4949-4965, 2011.
[12] C. Johnson, J.C. Nedelec, "On the coupling of boundary integral and finite element methods," *Mathematics of Computation*, vol. 35, pp. 1063-1079, 1980.
[13] R. MacCamy, S. Marin, "A finite element method for exterior interface problems," *International Journal of Mathematics and Mathematical Sciences*, vol. 3, pp. 311-350, 1980.
[14] H. Geng, Z. Xu, "Coupling of boundary integral equation and finite element methods for transmission problems in acoustics," *Numerical Algorithms*, vol. 82(2), pp. 479-501, 2019.
[15] T. Yin, A. Rathsfeld, L. Xu, "A BIE-based DtN-FEM for fluid-solid interaction problems," *Journal of Computational Mathematics*, vol. 36, pp. 47-69, 2018.
[16] H. Geng, T. Yin, L. Xu, "A priori error estimates of the DtN-FEM for the transmission problem in acoustics," *Journal of Computational and Applied Mathematics*, vol. 313, pp. 1-17, 2017.
[17] L. Xu, T. Yin, "Analysis of the Fourier series Dirichlet-to-Neumann boundary condition of the Helmholtz equation and its application to finite element methods," *Numerische Mathematik*, vol. 147, pp. 967-996, 2021.
[18] G. Grote, J. Keller, "On nonreflecting boundary conditions," *Journal of Computational physics*, vol. 122, pp. 231-243, 1995.
[19] T. Binford, D. Nicholls, N. Nigam,T. Warburtan, "Exact non-reflecting boundary conditions on perturbed domains and hp-finite elements," *Journal of Scientific Computing*, vol. 39, pp. 265-292, 2009.
[20] L. Chindelevitch, D. Nicholls, N. Nigam, "Error analysis and pre-conditioning for an enhanced DtN-FE algorithm for exterior scattering problems," *Journal of Computational and Applied Mathematics*, vol. 204, pp. 493-504, 2007.
[21] D. Nicholls, N. Nigma, "Exact non-reflecting boundary conditions on general domains," *Journal of Computational physics*, vol. 194, pp. 278-303, 2004.
[22] D. Nicholls, N. Nigma, "Error analysis of an enhanced DtN-FE method for exterior scattering problems," *Numerische Mathematik*, vol. 105, pp. 267-298, 2006.
[23] B. Engquist, A. Majda, "Absorbing boundary conditions for numerical simulation of waves," *Mathematics of Computation*, vol. 31, pp. 629-651, 1977.
[24] B. Engquist, A. Majda, "Radiation boundary conditions for acoustic and elastic wave calculations," *Communications on Pure and Applied Mathematics*, vol. 32, pp. 313-357, 1979.
[25] A. Bayliss, and E. Turkel, "Radiation boundary conditions for wave-like equations," *Communications on Pure and Applied Mathematics*, vol. 33, pp. 707-725, 1980.
[26] J.J. Shirron, I. Babuska, "A comparison of approximate boundary conditions and infinite element methods for exterior Helmholtz problems," *Computer Methods in Applied Mechanics and Engineering*, vol. 164, pp. 121-139, 1998.
[27] X. Wu, W. Chen, "Error estimates of the finite element method for interior transmission problems," *Journal of Scientific Computing*, vol. 57, pp. 331-348, 2013.
[28] T.S. Angell, R.E. Kleinman, and F. Hettlich, "The resistive and conductive problems for the exterior Helmholtz equation," *SIAM Journal on Applied Mathematics*, vol. 50, pp. 1607-1622, 1990.
[29] G.C. Hsiao, W. Wendland, "Boundary element methods: foundation and error analysis," *in: E. Stein, R. de Borst, T.J.R. Hughes (Eds.), in: Encyclopedia of Computational Mechanics*, John Wiley and Sons, Ltd., vol. 1, pp. 339-373, 2004.